Editors' Suggestion | Featured in Physics

Direct Characterization of Ultrafast Energy-Time Entangled Photon Pairs

Jean-Philippe W. MacLean,[1,2,*] John M. Donohue,[1,2,3] and Kevin J. Resch[1,2]
[1]Institute for Quantum Computing, University of Waterloo, Waterloo, Ontario Canada, N2L 3G1
[2]Department of Physics & Astronomy, University of Waterloo, Waterloo, Ontario Canada, N2L 3G1
[3]Integrated Quantum Optics, Applied Physics, University of Paderborn, 33098 Paderborn, Germany

(Received 31 October 2017; published 30 January 2018)

Energy-time entangled photons are critical in many quantum optical phenomena and have emerged as important elements in quantum information protocols. Entanglement in this degree of freedom often manifests itself on ultrafast time scales, making it very difficult to detect, whether one employs direct or interferometric techniques, as photon-counting detectors have insufficient time resolution. Here, we implement ultrafast photon counters based on nonlinear interactions and strong femtosecond laser pulses to probe energy-time entanglement in this important regime. Using this technique and single-photon spectrometers, we characterize all the spectral and temporal correlations of two entangled photons with femtosecond resolution. This enables the witnessing of energy-time entanglement using uncertainty relations and the direct observation of nonlocal dispersion cancellation on ultrafast time scales. These techniques are essential to understand and control the energy-time degree of freedom of light for ultrafast quantum optics.

DOI: 10.1103/PhysRevLett.120.053601

The energy-time degree of freedom of nonclassical light is of great interest for quantum information, as it supports various encodings, including frequency bins [1], time bins [2], and broadband temporal modes [3], and is intrinsically robust for propagation through long-distance fiber links [4]. Applications which harness quantum correlations in this degree of freedom, referred to as energy-time entanglement [5], include dispersion cancellation [6,7], high-dimensional quantum key distribution [8,9], and quantum-enhanced clock synchronization [10]. In ultrafast optics and attosecond physics, the ability to measure both frequency and temporal features has led to important innovations in electric field reconstruction techniques [11,12] and pulse characterization on very short time scales, enabling advances in spectroscopy [13], laser physics [14], nonlinear optics [15], and imaging [16]. In order to characterize and control energy-time entangled photons and advance biphoton pulse shaping, similar measurement capabilities are essential in the quantum regime.

Experimental signatures of entanglement can arise in correlation measurements of complementary variables [17], or through nonlocal quantum effects [5,6]. With the energy-time degree of freedom, one complementary set consists of measuring the intensity correlations as a function of the photon frequencies and as a function of their time of arrival. These have been individually realized for different photonic systems with measurements in frequency [18,19] or in time [20–22]. Certifying the presence of entanglement with direct measurements requires both spectral and temporal correlations, since acquiring only one remains insufficient to uniquely specify the other due to the ambiguity of the spectral phase. Depending on the platform, this can be challenging. Narrow-band photons from atomic systems can be readily measured in time but are difficult to spectrally resolve [22]. THz-bandwidth photons produced in spontaneous parametric down-conversion (SPDC) are often characterized spectrally, but they can have features on femtosecond time scales below current detector resolution [23].

Other techniques can be employed to infer the presence of energy-time entanglement. High-order interference effects with Franson interferometers have been used to illustrate entanglement between two [24] and three photons [25]. Nonlocal dispersion cancellation [6], whereby the temporal spread in coincidences remains unchanged when equal and opposite dispersion is applied to each photon, can also be used to witness entanglement [26,27]. For either method to be effective, the detector resolution must be shorter than the time scales of the correlations. Strong energy-time entanglement can nonetheless exist when the time scales of the correlations are shorter. Certain observations have pointed to nonlocal dispersion cancellation in this regime, but they either required introducing a very large amount of dispersion such that temporal resolution could be achieved with standard detectors [28], or used sum-frequency generation (SFG) between the photon pairs [29], which, unlike measurements with fast and independent detectors, has a close classical analogue [30]. Directly measuring ultrafast quantum effects requires new methods to control and analyze single photons in the time domain.

In nonlinear optics and laser physics, optical gating is widely used to overcome limitations with detectors which

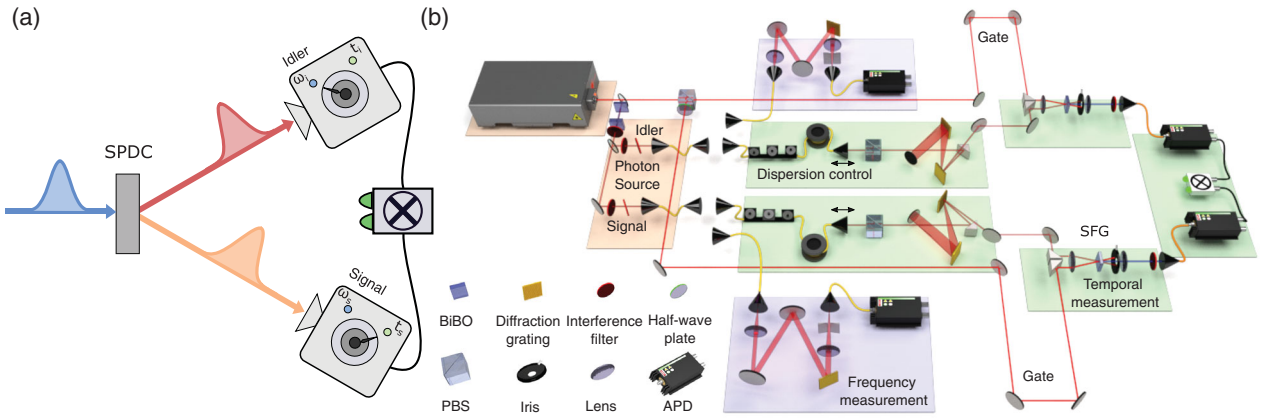

FIG. 1. Experimental setup. (a) Frequency-entangled photons are created through spontaneous parametric down-conversion of an ultrafast pulse from a frequency-doubled Ti:sapphire laser. Measurements of either the frequency or the time of arrival of each photon can be performed in coincidence. (b) Spectral measurements are made with dual single-photon monochromators. Temporal measurements are performed using optically gated single-photon detection. The gating is implemented via noncollinear sum-frequency generation between a strong gate pulse from the Ti:Sapph laser and the signal or idler. The dispersion of the signal and idler photons is controlled with a combination of single-mode fibers and grating compressors before the up-conversion. The up-converted signal is filtered with bandpass filters which remove the background second harmonic generation from the gate pulse. Temporal and frequency measurements are performed in coincidence to observe the spectral and temporal features of the photons.

are too slow to observe features on subpicosecond time scales. The gating is achieved by combining the signal with a short gate pulse in a nonlinear medium and measuring the up-conversion signal on the detector. With fast gates and slow detectors, an effective fast detector can be engineered to temporally resolve single photons [31,32] and photon pairs [20]. In this Letter, we develop fast optical gating to achieve subpicosecond timing resolution for spatially separated pairs of single photons. We use this technique in conjunction with single-photon spectrometers to explicitly measure both the spectral and temporal correlations of broadband photons, as well as the cross-correlations between the frequency of one photon and the time of arrival of the other. Furthermore, by controlling the dispersion of each photon, our high-resolution joint temporal measurements make it possible to directly observe nonlocal dispersion cancellation on femtosecond time scales.

Through spectral and temporal measurements, energy-time entanglement can be witnessed by violating uncertainty relations [33,34]. Two separable photons or classical pulses must satisfy the following inequality [17,21]:

$$\Delta(\omega_s + \omega_i)\Delta(t_s - t_i) \geq 1, \tag{1}$$

where each photon, labeled signal, and idler is described by its frequency ω and its time of arrival t, and Δ represents the standard deviation in the joint spectrum or joint temporal intensity. In other words, there is a nontrivial limit to the strength of the product of correlations between the sum of the frequencies and the difference in time of arrival if the photons are separable. However, this is not the case for energy-time entangled photons, where the right side of Eq. (1) can approach zero. Thus, the uncertainty relation is an entanglement witness.

Two-photon states produced via SPDC are usually energy-time entangled. In down-conversion, energy conservation tends to lead to entangled states with frequency anticorrelations, although dispersion engineered SPDC sources have been explored to produce photon pairs with uncorrelated [35,36] or even positively correlated frequencies [37–41]. For a pure state with no spectral phase, strong frequency correlations imply strong correlations in the time of arrival of the photons. Under these conditions, Eq. (1) can be violated, provided one has sufficient resolution in the measurements.

Our experimental setup is shown in Fig. 1. The laser output at 775 nm is frequency-doubled to 387.5 nm in 2 mm of bismuth-borate (BiBO). The resulting pump light is spectrally narrowed using a 0.085 nm $(1/\sqrt{e})$ bandpass filter. Signal and idler photon pairs are created through type-I SPDC of the pump in 5 mm of BiBO with central wavelengths of 729 nm and 827 nm, respectively. The bandwidths are controlled using tunable spectral edge filters, after which the photons are coupled to single-mode fibers. The fibers allow for easy switching between spectral measurement, temporal measurement, and direct detection. The dispersion of the fiber links is then compensated with grating-based pulse compressors. Spectral measurements are performed with grating-based scanning monochromators with a resolution of about 0.1 nm. Temporal measurements are performed through sum-frequency generation in 1 mm of type-I BiBO with a strong gate laser pulse with an intensity temporal width of 120 fs $(1/\sqrt{e})$, measured using an autocorrelation and assuming a Gaussian spectrum. The up-converted photons are detected after passing through

spectral bandpass filters which remove the second harmonic background of the gate pulse. Detection events for the signal and idler are measured in coincidence after they have passed through either both spectrometers, both temporal gates, or one of each. The corresponding measured joint spectrum, joint temporal intensity, and time-frequency plots, which measure the frequency of one photon in coincidence with the arrival time of the other, are shown in Fig. 2. Background subtraction has not been employed in the data [42].

The SFG employed in the temporal measurements can approach unit efficiency when the temporal duration of the photon is approximately the same length in time or shorter than the gate pulse [45]. However, in the present experiment, the photons are much longer than the gate, and consequently, we estimate a maximum up-conversion efficiency of approximately 30% [46]. The absolute efficiency of the temporal measurement apparatus at the cross-correlation peak, including fiber coupling, chirp compensation, and up-conversion, is found to be approximately 2% of this maximum.

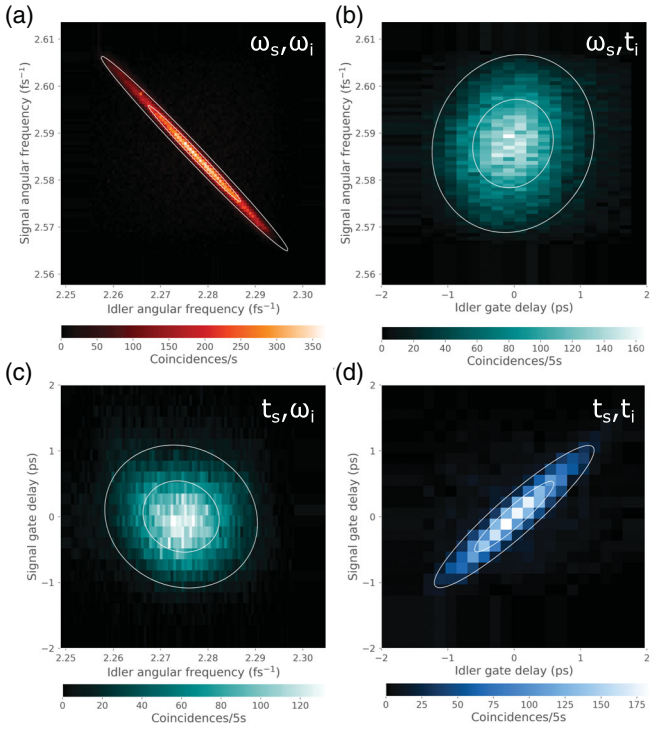

FIG. 2. Spectral and temporal characterization of ultrafast photons. A combination of spectral and temporal measurements are made in coincidence in order to measure (a) the joint spectrum, (d) the joint temporal intensity, as well as (b),(c) the cross-correlations between the time (frequency) of the idler and the frequency (time) of the signal. (a) Frequency anticorrelations with statistical correlation -0.9951 ± 0.0001 are accompanied with (d) positive correlations 0.987 ± 0.004 in the signal-idler arrival times. The time-frequency plots (b),(c) show little correlation—(0.111 ± 0.008) and (-0.106 ± 0.008), respectively—indicating low dispersion in the signal and idler photons. White lines on all plots correspond to 1σ and 2σ contours of two-dimensional Gaussian fits.

For each joint measurement of Fig. 2, the marginal width is obtained by fitting the marginals to a one-dimensional Gaussian, while the heralded width is obtained by taking the average of several slices of the data when the frequency or time of one photon is fixed. The statistical correlation, ρ, is obtained by finding the value that best fits a two-dimensional Gaussian with the measured marginals. Since the finite resolution of both spectral and temporal measurements are of the same order of magnitude as the spectral and temporal distributions, the measured features will be broadened. To account for this, the fit parameters are deconvolved assuming a Gaussian response function [41], and these values for the joint spectrum and joint temporal distribution of Figs. 2(a) and 2(d) are presented in Table I.

The measured joint spectrum shown in Fig. 2(a) exhibits strong anticorrelation (-0.9951 ± 0.0001) in the signal and idler frequencies, while the joint temporal intensity of Fig. 2(d) shows strong positive correlations (0.987 ± 0.004) in the arrival times of the photons. We can witness the effect of the spectral phase in Figs. 2(b) and 2(c), which show weak correlations between the frequency of one photon and the time of arrival of the other. Low correlations in the time-frequency plots may indicate little uncompensated dispersion in the experiment (see Supplemental Material [42]).

The spectral and timing correlations are further analyzed by binning the data presented in Figs. 2(a) and 2(d) into histograms based on $\omega_1 + \omega_2$ and $t_s - t_i$, as well as $\omega_s - \omega_i$ and $t_s + t_i$ for comparison, as shown in Fig. 3. The bin size was selected to match the step size of the measurement apparatus. Gaussian fits to the histograms give a joint uncertainty product $\Delta(\omega_s + \omega_i)\Delta(t_s - t_i) = (1.429 \pm 0.006\ \text{ps}^{-1})(0.203 \pm 0.005\ \text{ps}) = 0.290 \pm 0.007$, which violates the inequality of Eq. (1) by about 100

TABLE I. Ultrafast two-photon state parameters. Measured marginals, heralded widths, and correlations of the joint spectrum and joint temporal intensity are as presented in Figs. 2(a) and 2(d). All values are deconvolved to account for the finite resolution of the spectrometers and the temporal gate. Measured properties are widths in standard deviations, and error bars are calculated from Monte Carlo simulations assuming Poissonian noise. A more comprehensive list including both raw and deconvolved fit parameters can be found in the Supplemental Material [42].

Property	Joint spectrum	Joint temporal intensity
Signal marginal width	$(10.56 \pm 0.04)\ \text{ps}^{-1}$	(0.537 ± 0.009) ps
Signal heralded width	$(1.02 \pm 0.05)\ \text{ps}^{-1}$	(0.066 ± 0.018) ps
Idler marginal width	$(9.69 \pm 0.03)\ \text{ps}^{-1}$	(0.587 ± 0.015) ps
Idler heralded width	$(0.94 \pm 0.04)\ \text{ps}^{-1}$	(0.070 ± 0.019) ps
Correlation ρ	-0.9951 ± 0.0001	0.987 ± 0.004

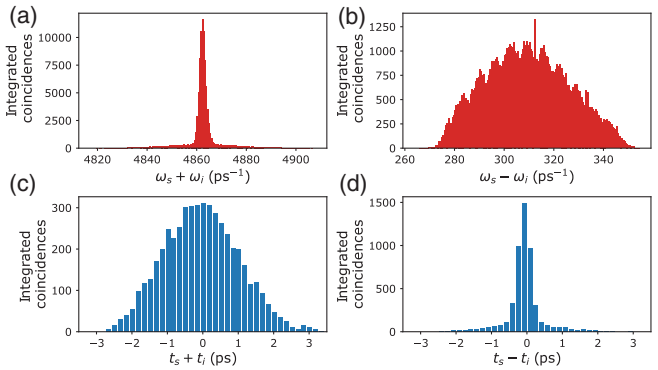

FIG. 3. Histograms of the frequency and time of arrival correlations between signal and idler photons. Coincidences are confined to a small region in (a) with $\Delta(\omega_s + \omega_i) = (1.429 \pm 0.006)$ ps^{-1} $(1.329 \pm 0.007$ ps^{-1} when corrected for the finite resolution of the gate), compared to (b) with $\Delta(\omega_s - \omega_i) = (18.16 \pm 0.05)$ ps^{-1} $(18.16 \pm 0.05$ ps$^{-1})$, indicating strong anticorrelations in frequency. Likewise, coincidences are localized in (d) with $\Delta(t_s - t_i) = 0.203 \pm 0.005$ ps $(0.110 \pm 0.010$ ps), compared to (c) with $\Delta(t_s + t_i) = 1.066 \pm 0.016$ ps $(1.052 \pm 0.016$ ps), corresponding to strong correlations in the time of arrival. From these values, we find a joint uncertainty product $\Delta(\omega_s + \omega_i)\Delta(t_s - t_i) = 0.290 \pm 0.007\,(0.15 \pm 0.01)$.

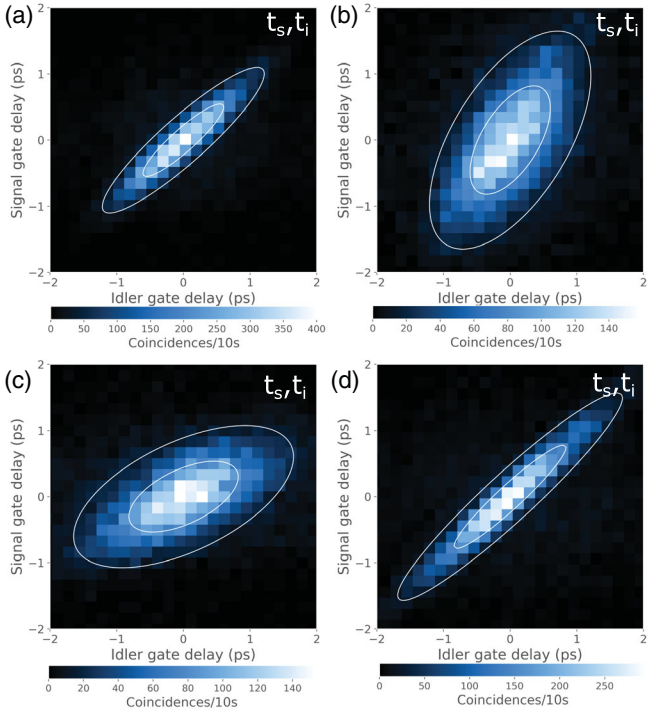

FIG. 4. Nonlocal dispersion cancellation observed in the joint temporal distributions. Joint temporal intensity for the signal and idler pair (a) without dispersion, (b) with a positive dispersion of $A_s = (0.0373 \pm 0.0015)$ ps^2 on the signal, (c) with a negative dispersion of $A_i = (-0.0359 \pm 0.0014)$ ps^2 on the idler, and (d) with both a positive dispersion of $A_s = (0.0373 \pm 0.0015)$ ps^2 on the signal and a negative dispersion of $A_i = (-0.0359 \pm 0.0014)$ ps^2 on the idler. For each, we measure the uncertainty in the difference in arrival times of the signal and idler $\Delta(t_s - t_i)$ and find (a) 0.235 ± 0.003 ps $(0.162 \pm 0.005$ ps when corrected for the finite resolution of the gate), (b) 0.708 ± 0.013 ps $(0.688 \pm 0.013$ ps), (c) 0.714 ± 0.010 ps $(0.693 \pm 0.011$ ps), (d) 0.245 ± 0.004 ps $(0.175 \pm 0.006$ ps). We witness nonlocal dispersion cancellation in the timing uncertainty $t_s - t_i$ in (d), as the width $\Delta(t_s - t_i)$ remains almost unchanged from the one measured in (a).

standard deviations. Error bars are obtained via Monte Carlo simulations assuming Poissonian noise. When deconvolved, we find $\Delta(\omega_s + \omega_i)\Delta(t_s - t_i) = (1.329 \pm 0.007\,\text{ps}^{-1})(0.110 \pm 0.010\,\text{ps}) = 0.15 \pm 0.01$. The measured uncertainty products thus provide a clear witness of energy-time entanglement on ultrafast time scales.

We now turn to the problem of measuring the impact of dispersion on our energy-time entangled state. We directly observe the effect of applied dispersion on the temporal correlations, as presented in the joint temporal intensities of Fig. 4. We control the spectral phase of the photons, $\phi(\omega_s, \omega_i) \approx A_s(\omega_s - \omega_{s0})^2 + A_i(\omega_i - \omega_{i0})^2$, with two grating compressors, where the chirp parameters A_s and A_i are for the signal and idler fields, respectively. We estimate the magnitude of the applied dispersion from the geometry of the compressor and the relative position of the gratings [47], and measure the standard deviation $\Delta(t_s - t_i)$ of a Gaussian fit from histograms of $t_s - t_i$.

Starting from the case with no dispersion [Fig. 4(a)], we apply positive dispersion $A_s = (0.0373 \pm 0.0015)$ ps^2 to only the signal [Fig. 4(b)] and negative dispersion $A_i = -(0.0359 \pm 0.0014)$ ps^2 to only the idler [Fig. 4(c)]. In these two cases, we observe a large increase in the timing uncertainty $\Delta(t_s - t_i)$ and a vertical or horizontal shear of the joint-temporal intensity along the corresponding axis. We then apply the same amount of positive and negative dispersion to the signal and idler as before [Fig. 4(d)], where the dispersion applied to the idler is set to minimize the timing uncertainty between the two photons. Here, the timing uncertainty in arrival time $\Delta(t_s - t_i)$ is almost unchanged. This is the signature of nonlocal dispersion cancellation, limited by the finite correlations of the initial two-photon state (see Supplemental Material [42]). The temporal marginals in Fig. 4(d) still increase, since each side remains exposed to a significant amount of dispersion.

For classical pulses, the effect of dispersion on the correlations in arrival times can be expressed as an inequality [26], $\Delta(t_s - t_i)_F^2 \geq \Delta(t_s - t_i)_0^2 + 4A^2/\Delta(t_s - t_i)_0^2$, where $\Delta(t_s - t_i)_0$ is the initial difference in detection times, and $\Delta(t_s - t_i)_F$ is the final difference with equal and opposite dispersion A applied on each side. Under the assumption that the initial state is unchirped, taking the measured initial value from Fig. 4(a), $\Delta(t_s - t_i)_0 = 0.235$ ps (0.162 ps when corrected for the gate resolution), and using the average magnitude of the applied dispersion $A = 0.0366$ ps^2, we calculate that the standard deviation in

arrival times for classical pulses has to be at least $\Delta(t_s - t_i)_F \geq 0.390$ ps (0.480 ps). However, the measured uncertainty observed in Fig. 4(d), $\Delta(t_s - t_i) = (0.245 \pm 0.004)$ ps, remains significantly smaller. The experimental apparatus thus provides a direct way to detect this inherently quantum effect in a regime inaccessible to current detectors.

We have directly measured both the temporal and frequency correlations of an ultrafast biphoton pulse. Optical gating employed here was critical for realizing ultrafast coincidence detection and correspondingly high-resolution temporal measurements. We observe energy-time entanglement via a joint time-bandwidth inequality and demonstrate ultrafast nonlocal dispersion cancellation of the biphotons with direct and independent detection. This work can be extended to quantum interference measurements on ultrafast time scales, and can be combined with temporal imaging to greatly increase the versatility of energy-time entangled photons for quantum information applications.

The authors thank M. Mazurek for fruitful discussions and M. Mastrovich for valuable assistance in the laboratory. This research was supported in part by the Natural Sciences and Engineering Research Council of Canada (NSERC), Canada Research Chairs, Industry Canada, and the Canada Foundation for Innovation (CFI).

*jpmaclean@uwaterloo.ca

[1] S. Ramelow, L. Ratschbacher, A. Fedrizzi, N. K. Langford, and A. Zeilinger, Phys. Rev. Lett. **103**, 253601 (2009).
[2] I. Marcikic, H. de Riedmatten, W. Tittel, V. Scarani, H. Zbinden, and N. Gisin, Phys. Rev. A **66**, 062308 (2002).
[3] B. Brecht, D. V. Reddy, C. Silberhorn, and M. G. Raymer, Phys. Rev. X **5**, 041017 (2015).
[4] Q. Zhang, H. Takesue, S. W. Nam, C. Langrock, X. Xie, B. Baek, M. M. Fejer, and Y. Yamamoto, Opt. Express **16**, 5776 (2008).
[5] J. D. Franson, Phys. Rev. Lett. **62**, 2205 (1989).
[6] J. D. Franson, Phys. Rev. A **45**, 3126 (1992).
[7] A. M. Steinberg, P. G. Kwiat, and R. Y. Chiao, Phys. Rev. Lett. **68**, 2421 (1992).
[8] J. Nunn, L. J. Wright, C. Sller, L. Zhang, I. A. Walmsley, and B. J. Smith, Opt. Express **21**, 15959 (2013).
[9] J. M. Lukens, A. Dezfooliyan, C. Langrock, M. M. Fejer, D. E. Leaird, and A. M. Weiner, Phys. Rev. Lett. **112**, 133602 (2014).
[10] V. Giovannetti, S. Lloyd, and L. Maccone, Nature (London) **412**, 417 (2001).
[11] R. Trebino, K. W. DeLong, D. N. Fittinghoff, J. N. Sweetser, M. A. Krumbgel, B. A. Richman, and D. J. Kane, Rev. Sci. Instrum. **68**, 3277 (1997).
[12] I. A. Walmsley and C. Dorrer, Adv. Opt. Photonics **1**, 308 (2009).
[13] A. H. Zewail, J. Phys. Chem. A **104**, 5660 (2000).
[14] S.-W. Bahk, P. Rousseau, T. A. Planchon, V. Chvykov, G. Kalintchenko, A. Maksimchuk, G. A. Mourou, and V. Yanovsky, Opt. Lett. **29**, 2837 (2004).
[15] Z. Chang, A. Rundquist, H. Wang, M. M. Murnane, and H. C. Kapteyn, Phys. Rev. Lett. **79**, 2967 (1997).
[16] W. R. Zipfel, R. M. Williams, and W. W. Webb, Nat. Biotechnol. **21**, 1369 (2003).
[17] S. Mancini, V. Giovannetti, D. Vitali, and P. Tombesi, Phys. Rev. Lett. **88**, 120401 (2002).
[18] M. Avenhaus, A. Eckstein, P. J. Mosley, and C. Silberhorn, Opt. Lett. **34**, 2873 (2009).
[19] S. Schwarz, B. Bessire, and A. Stefanov, Int. J. Quantum. Inform. **12**, 1560026 (2014).
[20] O. Kuzucu, F. N. C. Wong, S. Kurimura, and S. Tovstonog, Phys. Rev. Lett. **101**, 153602 (2008).
[21] L. K. Shalm, D. R. Hamel, Z. Yan, C. Simon, K. J. Resch, and T. Jennewein, Nat. Phys. **9**, 19 (2013).
[22] Y.-W. Cho, K.-K. Park, J.-C. Lee, and Y.-H. Kim, Phys. Rev. Lett. **113**, 063602 (2014).
[23] M. D. Eisaman, J. Fan, A. Migdall, and S. V. Polyakov, Rev. Sci. Instrum. **82**, 071101 (2011).
[24] P. G. Kwiat, A. M. Steinberg, and R. Y. Chiao, Phys. Rev. A **47**, R2472 (1993).
[25] S. Agne, T. Kauten, J. Jin, E. Meyer-Scott, J. Z. Salvail, D. R. Hamel, K. J. Resch, G. Weihs, and T. Jennewein, Phys. Rev. Lett. **118**, 153602 (2017).
[26] T. Wasak, P. Szankowski, W. Wasilewski, and K. Banaszek, Phys. Rev. A **82**, 052120 (2010).
[27] J. A. Jaramillo-Villegas, P. Imany, O. D. Odele, D. E. Leaird, Z.-Y. Ou, M. Qi, and A. M. Weiner, Optica **4**, 655 (2017).
[28] S.-Y. Baek, Y.-W. Cho, and Y.-H. Kim, Opt. Express **17**, 19241 (2009).
[29] K. A. O'Donnell, Phys. Rev. Lett. **106**, 063601 (2011).
[30] R. Prevedel, K. M. Schreiter, J. Lavoie, and K. J. Resch, Phys. Rev. A **84**, 051803 (2011).
[31] O. Kuzucu, F. N. Wong, S. Kurimura, and S. Tovstonog, Opt. Lett. **33**, 2257 (2008).
[32] M. Allgaier, G. Vigh, V. Ansari, C. Eigner, V. Quiring, R. Ricken, B. Brecht, and C. Silberhorn, Quantum Sci. Technol. **2**, 034012 (2017).
[33] J. C. Howell, R. S. Bennink, S. J. Bentley, and R. W. Boyd, Phys. Rev. Lett. **92**, 210403 (2004).
[34] M. Edgar, D. Tasca, F. Izdebski, R. Warburton, J. Leach, M. Agnew, G. Buller, R. Boyd, and M. Padgett, Nat. Commun. **3**, 984 (2012).
[35] P. J. Mosley, J. S. Lundeen, B. J. Smith, P. Wasylczyk, A. B. U'Ren, C. Silberhorn, and I. A. Walmsley, Phys. Rev. Lett. **100**, 133601 (2008).
[36] C. Chen, C. Bo, M. Y. Niu, F. Xu, Z. Zhang, J. H. Shapiro, and F. N. C. Wong, Opt. Express **25**, 7300 (2017).
[37] W. P. Grice and I. A. Walmsley, Phys. Rev. A **56**, 1627 (1997).
[38] W. P. Grice, A. B. U'Ren, and I. A. Walmsley, Phys. Rev. A **64**, 063815 (2001).
[39] A. Eckstein, A. Christ, P. J. Mosley, and C. Silberhorn, Phys. Rev. Lett. **106**, 013603 (2011).
[40] G. Harder, V. Ansari, B. Brecht, T. Dirmeier, C. Marquardt, and C. Silberhorn, Opt. Express **21**, 13975 (2013).
[41] J. M. Donohue, M. Mastrovich, and K. J. Resch, Phys. Rev. Lett. **117**, 243602 (2016).

[42] See Supplemental Material at http://link.aps.org/supplemental/10.1103/PhysRevLett.120.053601 for additional experimental details and results, which includes Refs. [43,44].
[43] R. Hanbury Brown and R. Q. Twiss, Nature (London) **178**, 1046 (1956).
[44] B. Brecht and C. Silberhorn, Phys. Rev. A **87**, 053810 (2013).
[45] A. P. Vandevender and P. G. Kwiat, J. Mod. Opt. **51**, 1433 (2004).
[46] J. M. Donohue, M. D. Mazurek, and K. J. Resch, Phys. Rev. A **91**, 033809 (2015).
[47] E. Treacy, IEEE J. Quantum Electron. **5**, 454 (1969).